Published in final edited form as:
Nature. 2013 February 14; 494(7436): 247–250. doi:10.1038/nature11826.

In vitro expansion of single Lgr5+ liver stem cells induced by Wnt-driven regeneration

Meritxell Huch[1,*], **Craig Dorrell**[3,*], **Sylvia F. Boj**[1], **Johan H. van Es**[1], **Marc van de Wetering**[1], **Vivian S.W. Li**[1], **Karien Hamer**[1], **Nobuo Sasaki**[1], **Milton J. Finegold**[4], **Annelise Haft**[3], **Markus Grompe**[3], and **Hans Clevers**[1,5]

[1]Hubrecht Institute for Developmental Biology and Stem Cell Research, Uppsalalaan 8, 3584CT Utrecht & University Medical Centre Utrecht, Netherlands [3]Oregon Stem Cell Center, Papé Family Pediatric Research Institute, Oregon Health and Science University, Portland, Oregon 97239, USA [4]Department of Pathology, Texas children's Hospital, Houston, Texas 77030 USA

Abstract

The Wnt target gene *Lgr5* marks actively dividing stem cells in Wnt-driven, self-renewing tissues such as small intestine and colon[1], stomach[2] and hair follicles[3]. A 3D culture system allows long-term clonal expansion of single Lgr5$^+$ stem cells into transplantable organoids that retain many characteristics of the original epithelial architecture[2, 4, 5]. A crucial component of the culture medium is the Wnt agonist Rspo1[6], the recently discovered ligand of Lgr5[7, 8]. Here we show that *Lgr5-LacZ* is not expressed in healthy adult liver, yet that small Lgr5-LacZ$^+$ cells appear near bile ducts upon damage, coinciding with robust activation of Wnt signaling. As shown by lineage tracing using a novel *Lgr5-ires-CreERT2* knock-in allele, damage-induced Lgr5$^+$ cells generate hepatocytes and bile ducts *in vivo*. Single Lgr5$^+$ cells from damaged liver can be clonally expanded as organoids in Rspo1-based culture medium over multiple months. Such clonal organoids can be induced to differentiate *in vitro* and to generate functional hepatocytes upon transplantation into FAH$^{-/-}$ mice. These findings imply that previous observations on Lgr5$^+$ stem cells in actively self-renewing tissues extend to damage-induced stem cells in a tissue with a low rate of spontaneous proliferation.

Quiescent stem cells are believed to reside in biliary ducts[9]. Sox9- and Foxl1-based lineage tracing have proven the existence of such cells[10–13]. In the adult liver, the Wnt pathway is exclusively active in hepatocytes that surround central veins (perivenous hepatocytes)[14]. In

[5]Corresponding author: Hans Clevers, Hubrecht Institute & University Medical Centre Utrecht, Uppsalalaan 8, 3584CT Utrecht, Netherlands, h.clevers@hubrecht.eu, Phone: 31 30 2121800, Fax: 31 30 2121801.
[*]Equal contribution.

Supplementary Information is linked to the online version of the paper at www.nature.com/nature.

Author Contributions

Experiments were conceived and designed by MH, CD, MG and HC. Experiments were performed by MH, CD, SFB, MvdW, VSWL, NS, KH and AH. MH analyzed the data. JHvE designed and generated the *Lgr5-ires-CreERT2* allele. VSWL performed the bioinformatic analysis of the microarrays and MJF the Y-chromosome staining. MH and HC wrote the manuscript.

Author Information

The data for the microarray analysis have been deposited to the Gene Expression Omnibus under the accession number GSE32210. Reprints and permissions information is available at www.nature.com/reprints. The authors declare competing financial interests: details accompany the full-text HTML version of the paper at www.nature.com/nature. Readers are welcome to comment on the online version of this article at www.nature.com/nature. Correspondence and requests for materials should be addressed to H.C. (h.clevers@hubrecht.eu).

Competing Financial Interests

MH & HC are inventors on a patent application related to this work.

bile ducts, Wnt signaling becomes active following liver injury[15]. Accordingly, activity of the generic Wnt reporter *Axin2-LacZ*[16] was detected only in perivenous hepatocytes, and was upregulated upon induction of liver injury by CCl_4 injection[17] (Supplementary Fig. 1a–b). Maximal expression occurred between day 3–6 after damage (Supplementary Fig. 1c). By microarray analysis, we noted induction of Wnt6 (>2 fold), of several Rspondins (3–6 fold) and of many Wnt target genes previously characterized in intestinal crypt cells[8], including *Lgr5* (≥2 fold). Notably, perivenous hepatocyte Wnt target genes (*Glul, Slc1a2, Rhbg, Cyp1a2*)[14] were downregulated, implying that Wnt activation occurred outside perivenous hepatocytes (Supplementary Fig. 1d; Supplementary Table 1).

In untreated *Lgr5-LacZ* knock-in mice[1], *Lgr5-LacZ* expression was essentially undetectable (Fig. 1a). Upon CCl_4 treatment, clear reporter activity (peaking at day 5–6) occurred in groups of small cells (Fig. 1b and Supplementary Fig. 2a–c). These $Lgr5^+$ cells expressed *Sox9*, a relatively broad ductal progenitor marker[10,12–13], but no mature hepatocyte or stellate cell markers (Supplementary Fig. 2d–f). The gene expression profile of CCl_4-induced $Lgr5^+$ cells correlated closely with biliary duct cells but not hepatocytes (Supplementary Fig. 1g). Closer comparison with the biliary duct profile revealed that multiple Wnt target genes and multiple intestinal Lgr5 stem cell genes were enriched in liver $Lgr5^+$ cells ([18]; (Supplementary Fig. 2g and Supplementary Tables 2–3).

We then aimed to visualize Lgr5 progeny by lineage tracing. The *Lgr5-EGFP-ires-CreERT2* allele[1] is permanently silenced in liver. Therefore, we generated a new *Lgr5* allele by inserting *iresCreERT2* into its 3′UTR (Supplementary Fig. 3a), and we crossed these mice with the *R26R-LacZ* reporter[19]. After a single tamoxifen injection, tracing events were readily detected in the intestine, validating this allele (Supplementary Fig. 3b). Adult offspring were treated with CCl_4 and, 5 days later, Cre activity was activated by tamoxifen. Two days after tamoxifen induction, groups of small, proliferative $LacZ^+$ cells became visible that evolved into fully mature hepatocytes from day 7 onwards (Fig. 1c). Since CCl_4 induces central vein damage, we also tested two ‘oval cell response’-models: MCDE (methionine choline-deficient diet supplemented with ethionine)[20] and DDC (3,5-diethoxycarbonyl-1,4-dihydrocollidine)[21]. In both models, tracing of hepatocytes and biliary ducts were readily detected (Fig. 2d and Supplementary Fig. 3d–f). In the absence of liver damage, no tracing events were detected in the livers of mice with the same genotype (Supplementary Fig. 3c). Similar tracing data have been reported for *Foxl1*[13, 11].

Given the expression of the Wnt-dependent Lgr5 stem cell marker, we reasoned that adult liver progenitors could possibly be expanded from the ductal compartment under our previously defined organoid culture conditions[2,4]. Previously established liver culture methods typically yield cell populations that undergo senescence over time[10,13,22–24] unless the cells are transformed. To establish liver progenitor cultures, biliary duct fragments were embedded in Matrigel containing the ‘generic’ organoid culture factors EGF and Rspo1[4], to which FGF10, HGF and Nicotinamide (Expansion Medium, EM) were added. Virtually all fragments formed cysts that grew into much larger liver organoids (Supplementary Fig. 4a–b), expressing *Lgr5* and ductal markers (Supplementary Fig. 4c). Without EGF, Rspo1 or Nicotinamide, the cultures deteriorated within 1–2 passages (Supplementary Fig. 4d). Cultures have been maintained more than 12 months, by weekly passaging at 1:8. We then initiated single cell (clonal) cultures from Lgr5-$LacZ^+$ cells, FACS-sorted from *Lgr5-LacZ* mice after a single dose of CCl_4 (Fig. 2a–b). Sorted cells cultured in our defined EM conditions rapidly divided and formed cyst-like structures that were maintained for >8 months by weekly passaging 1:8 (Fig. 2c and Supplementary Fig. 5e). Karyotypic analysis of both clonal and bulk cultures, revealed that the majority of cells (~85%) harbored normal chromosome numbers, even at 8 months (Supplementary Fig. 4e), consistent with the ~25% level of aneuploidy in young adult mouse liver[25]. Importantly, secondary cultures from

Lgr5-LacZ^{+} cells could also be established that could be expanded for >4 months in culture (Supplementary Fig. 5a–e).

To assess the lineage potential of Lgr5 cells, we performed gene expression profiling of clonal organoids. Microarray analysis revealed that clonal organoids resembled adult liver. *Lgr5*, and progenitor markers such as *Sox9*, *Cd44* and *Prom1*[10] were highly upregulated. The clonal organoids expressed multiple hepatocyte-lineage markers as well as bile duct markers, implying that single Lgr5 cells are bi-potential (Supplementary Fig. 6a–f). Markers of mature hepatocytes were only weakly expressed or absent (Supplementary Fig. 7a, EM column).

Marker analysis suggested that the culture conditions were biased towards induction of a biliary cell fate. To induce hepatocyte maturation *in vitro*, we defined a Differentiation Medium (DM). Inhibition of Notch and TGFβ signaling, both implicated in biliary cell fate determination *in vivo*[26–27], induced the expression of ~200 genes. These included *Tbx3, PPARγ,* and *BMP2,* essential for liver maturation[27–29], as well as mature hepatocyte markers such as *Cyp3a11, Fah, G6p* and *Alb* (Supplementary Fig. 7a–b). We also observed induction of a set of genes involved in cholesterol and lipid metabolism, and genes encoding p450 cytochromes (Supplementary Fig. 7c–d). Accordingly, the progenitor profile was shut down, as evidenced by downregulation of *Lgr5* (Supplementary Fig. 7a, DM column). Immunofluorescent staining revealed the expression of Hnf4a and Albumin, as well as the basolateral membrane protein Mrp4 and the tight junction protein Zo-1 (Fig. 3a–d). Up to 33% of the cells were positive for the OC2-2F8 hepatocyte marker and displayed high granularity by flow cytometry analysis, a feature of mature hepatocytes (Fig. 3d and Supplementary Fig. 7e). Bi-nucleation, a hallmark of hepatocyte maturation, was also detected (Supplementary Fig. 7f). Of note, the ductal phenotype was not fully abolished, as patches of Krt19-positive cells remained present (Fig. 4d). The differentiated organoids were subjected to several tests for hepatocyte function. Around 90% of the cells were competent for LDL-uptake (Fig. 4e–f) and accumulated glycogen (Fig. 4g). Abundant amounts of albumin were secreted into the medium (Fig. 4h), while hepatocyte cytochrome p450 function was induced (Fig. 4i). Yet, these *in vitro* functions remained less pronounced than those of freshly isolated hepatocytes.

We then transplanted organoids from 3 independent clones into *fumarylacetoacetate hydrolase (FAH)*$^{-/-}$ mutant mice, a model for Tyrosinemia type I liver disease. Deficiency of FAH results in liver failure unless the mice are administered NTBC (2-(2-nitro-4-trifluoro-methylbenzyol)-1,3-cyclohexanedione)[30]. Organoids derived from single Lgr5^{+} cells expanded in EM, were differentiated in DM for 9 days and cell suspensions were intrasplenically injected in the mice (Fig. 4a). At 2–3 months post-transplantation, we analyzed engraftment by FAH staining on serial sections of the entire liver of 15 recipient mice. We found FAH^{+} nodules (Fig. 4b and Supplementary. Fig. 9a–d), which occupied ~1% of the liver parenchyma, in 2 out of 5 mice transplanted with clone I and 2 out of 5 mice transplanted with clone III. For clone II, we only detect FAH+ hepatocytes in 1 out of 5 mice analyzed, in an area that occupied 0.1% of the total liver volume.

The histological results were confirmed by PCR analysis for the donor-cell gene *LacZ* (Supplementary Fig. 9e). Histologically, the FAH^{+} patches consisted of cells with hepatocyte morphology, HNF4α positive and *Krt19* negative (Fig. 4c–d). This indicated that, *in vivo*, the cells had acquired a fully mature hepatocyte phenotype, while silencing any remaining ductal expression. No fusion of organoid cells with host hepatocytes was observed (Supplementary Fig. 9f). For comparison, transplantation of oval cells (MIC1-1C3^{+}/133^{+}/26^{-}/CD45^{-}/11b^{-}/31^{-}) has only resulted in trace engraftment (<0.1% of the total liver) in 2 out of 20 *Fah*$^{-/-}$ mice[10]. We compared the survival rate of the engrafted

mice (graft+) to the non-engrafted mice (transplanted mice, negative for FAH staining, graft-) and to the non-transplanted controls (Fig. 4e). We observed a significant increase in survival of the graft+ group compared to the graft- group (log rank=0.02) and to the non-transplanted group (log rank=0.007), indicating that the transplanted cells contributed to liver function *in vivo*. Unlike typical results obtained upon transplantation of freshly isolated hepatocytes, where >30% of the liver repopulates and functional rescue is near 100%[30], we did not observe a full rescue of the enzymatic defect, in concordance with the limited contribution of the transplanted areas to overall liver volume. Such rescue will depend on further optimization of the differentiation and transplantation protocols. Competitive transplantations assays comparing normal hepatocytes to Lgr5-derived cells may reveal further phenotypic characteristics of the latter. Importantly, no dysplastic or anaplastic growth was detected in any of the recipient mice.

In conclusion, we report that damage of adult liver results in the expression of *Lgr5* in small cells near bile ducts. By lineage tracing, these cells generate significant numbers of hepatocytes and biliary duct cells during the repair phase. The small $Lgr5^+$ cells express multiple Wnt target genes and other markers of intestinal $Lgr5^+$ stem cells. Yet, they carry the hallmarks of bi-potent liver progenitors. Thus, *Lgr5* not only marks Wnt-driven stem cells that drive constitutive (intestine, stomach) or intermittent (hair follicle) physiological tissue self-renewal, but also defines a class of stem cells/progenitors that is called into action upon tissue damage. The Wnt-driven regenerative response can be exploited *in vitro* to expand freshly isolated duct fragments or even single $Lgr5^+$ cells into transplantable organoids. The Rspo1-Lgr5 axis is crucial to the long-term growth and the observed genetic and phenotypic stability of the resulting organoids. Thus, the Rspo1-Lgr5 axis allows adult stem cells to expand extensively in culture, like embryonic stem cells do. Our observations may serve as the basis for the development of regenerative strategies using adult stem/progenitor cells obtained from solid organs. Since these approaches can be based on the *in vitro* expansion of a single adult Lgr5 progenitor cell, specific and safe genetic modifications may become feasible.

Methods Summary

Mouse experiments

Animal experiments were performed in accordance with the institutional review committee at Hubrecht Institute and Oregon Health & Science University (IS00000119). Generation and genotyping of the *Lgr5-LacZ* and *Fah*$^{-/-}$*/Rag2*$^{-/-}$*/Il2R*$\gamma^{-/-}$ *(FGR)* mice have been previously described[1, 30]. *Axin2-LacZ* mice were obtained from EMMA (Germany). To induce liver injury, 3–5 months-old *Lgr5-LacZ, Axin2-LacZ, Lgr5-ires-CreERT2 x Rosa26LacZ* or WT littermate BL6/Balb-c F1 mice received an intraperitoneal injection of CCl_4 (1ml/kg, Sigma) dissolved in corn oil, or corn oil alone. *Lgr5-ires-CreERT2 x Rosa26LacZ* were fed with a diet supplemented with 0.1% (w/w) DDC or supplemented with MCD and 0.1% ethionine in the drinking water (MCDE) or with regular diet (not supplemented). Four or five days after liver injury, lineage tracing was induced by 1 or 2 IP injections of tamoxifen (3mg/mouse). Detailed lineage tracing protocols are provided in Supplementary Methods.

Liver organoid culture

Biliary ducts or sorted *Lgr5-LacZ+* cells were isolated, mixed with Matrigel (BD Bioscience) and cultured as described in ref. 2. Medium composition was AdDMEM/F12 (Invitrogen) supplemented with B27 and N2 (Invitrogen), N-Acetylcysteine (1.25 μM, Sigma), gastrin (10 nM, Sigma), EGF (50 ng/ml, Peprotech), 10% RSPO1 Conditioned Medium (kindly provided by Calvin Kuo), FGF10 (100 ng/ml, Peprotech), nicotinamide (10

mM, Sigma) and HGF (50 ng/ml, Peprotech). Detailed protocols are provided in Supplementary Methods.

Transplantation assay

Three *Lgr5*-derived single cell clones were grown for at least 3 months and differentiated for 9 days prior to transplant to *Fah*$^{-/-}$/*Rag2*$^{-/-}$/*Il2Rγ*$^{-/-}$ mice (intrasplenic injection). Detailed protocols are provided in Supplementary Methods.

Supplementary Material

Refer to Web version on PubMed Central for supplementary material.

Acknowledgments

We thank Harry Begthel, Annemarie Buijs, Wouter Karthaus, Carla Kroon-Veenboer, Maaike van den Born, Stieneke van der Brink, and Laura Zeinstra for technical assistance. This work was supported by grants to MH (EU/236954) and SFB (EU/232814), VSWL and JHvE (Ti Pharma/T3-106).

References

1. Barker N, et al. Identification of stem cells in small intestine and colon by marker gene Lgr5. Nature. 2007; 449:1003–1007. [PubMed: 17934449]
2. Barker N, et al. Lgr5(+ve) stem cells drive self-renewal in the stomach and build long-lived gastric units in vitro. Cell Stem Cell. 2010; 6:25–36. [PubMed: 20085740]
3. Jaks V, et al. Lgr5 marks cycling, yet long-lived, hair follicle stem cells. Nat Genet. 2008; 40:1291–1299. [PubMed: 18849992]
4. Sato T, et al. Single Lgr5 stem cells build crypt-villus structures in vitro without a mesenchymal niche. Nature. 2009; 459:262–265. [PubMed: 19329995]
5. Yui S, et al. Functional engraftment of colon epithelium expanded in vitro from a single adult Lgr5(+) stem cell. Nat Med. 2012; 18:618–623. [PubMed: 22406745]
6. Kim KA, et al. Mitogenic influence of human R-spondin1 on the intestinal epithelium. Science. 2005; 309:1256–1259. [PubMed: 16109882]
7. Carmon KS, Gong X, Lin Q, Thomas A, Liu Q. R-spondins function as ligands of the orphan receptors LGR4 and LGR5 to regulate Wnt/beta-catenin signaling. Proc Natl Acad Sci USA. 2011; 108:11452–11457. [PubMed: 21693646]
8. de Lau W, et al. Lgr5 homologues associate with Wnt receptors and mediate R-spondin signalling. Nature. 2011; 476:293–297. [PubMed: 21727895]
9. Duncan AW, Dorrell C, Grompe M. Stem cells and liver regeneration. Gastroenterology. 2009; 137:466–481. [PubMed: 19470389]
10. Dorrell C, et al. Prospective isolation of a bipotential clonogenic liver progenitor cell in adult mice. Gene Dev. 2011; 25:1193–1203. [PubMed: 21632826]
11. Sackett SD, et al. Foxl1 is a marker of bipotential hepatic progenitor cells in mice. Hepatology. 2009; 49:920–929. [PubMed: 19105206]
12. Furuyama K, et al. Continuous cell supply from a Sox9-expressing progenitor zone in adult liver, exocrine pancreas and intestine. Nat Genet. 2011; 43:34–41. [PubMed: 21113154]
13. Shin S, et al. Foxl1-Cre-marked adult hepatic progenitors have clonogenic and bilineage differentiation potential. Gene Dev. 2011; 25:1185–1192. [PubMed: 21632825]
14. Benhamouche S, et al. Apc tumor suppressor gene is the “zonation-keeper” of mouse liver. Dev Cell. 2006; 10:759–770. [PubMed: 16740478]
15. Hu M, et al. Wnt/beta-catenin signaling in murine hepatic transit amplifying progenitor cells. Gastroenterology. 2007; 133:1579–1591. [PubMed: 17983805]
16. Lustig B, et al. Negative feedback loop of Wnt signaling through upregulation of conductin/axin2 in colorectal and liver tumors. Mol Cell Biol. 2002; 22:1184–1193. [PubMed: 11809809]

17. Stowell RE, Lee CS. Histochemical studies of mouse liver after single feeding of carbon tetrachloride. AMA Arch Pathol. 1950; 50:519–537. [PubMed: 14770716]
18. Munoz J, et al. The Lgr5 intestinal stem cell signature: robust expression of proposed quiescent '+4' cell markers. The EMBO journal. 2012; 31:3079–3091. [PubMed: 22692129]
19. Soriano P. Generalized lacZ expression with the ROSA26 Cre reporter strain. Nat Genet. 1999; 21:70–71. [PubMed: 9916792]
20. Akhurst B, et al. A modified choline-deficient, ethionine-supplemented diet protocol effectively induces oval cells in mouse liver. Hepatology. 2001; 34:519–522. [PubMed: 11526537]
21. Preisegger KH, et al. Atypical ductular proliferation and its inhibition by transforming growth factor beta1 in the 3,5-diethoxycarbonyl-1,4-dihydrocollidine mouse model for chronic alcoholic liver disease. Laboratory investigation; a journal of technical methods and pathology. 1999; 79:103–109.
22. Michalopoulos GK, Bowen WC, Mulè K, Stolz DB. Histological organization in hepatocyte organoid cultures. Am J Pathol. 2001; 159:1877–1887. [PubMed: 11696448]
23. Schmelzer E, et al. Human hepatic stem cells from fetal and postnatal donors. J Exp Med. 2007; 204:1973–1987. [PubMed: 17664288]
24. Kamiya A, Kakinuma S, Yamazaki Y, Nakauchi H. Enrichment and clonal culture of progenitor cells during mouse postnatal liver development in mice. Gastroenterology. 2009; 137:1114–1126. [PubMed: 19524574]
25. Duncan AW, et al. The ploidy conveyor of mature hepatocytes as a source of genetic variation. Nature. 2010; 467:707–710. [PubMed: 20861837]
26. Tanimizu N, Miyajima A. Notch signaling controls hepatoblast differentiation by altering the expression of liver-enriched transcription factors. J Cell Sci. 2004; 117:3165–3174. [PubMed: 15226394]
27. Lemaigre FP. Mechanisms of liver development: concepts for understanding liver disorders and design of novel therapies. Gastroenterology. 2009; 137:62–79. [PubMed: 19328801]
28. Zaret KS. Genetic programming of liver and pancreas progenitors: lessons for stem-cell differentiation. Nat Rev Genet. 2008; 9:329–340. [PubMed: 18398419]
29. Si-Tayeb K, Lemaigre FP, Duncan SA. Organogenesis and development of the liver. Dev Cell. 2010; 18:175–189. [PubMed: 20159590]
30. Azuma H, et al. Robust expansion of human hepatocytes in Fah−/−/Rag2−/−/Il2rg−/− mice. Nat Biotechnol. 2007; 25:903–910. [PubMed: 17664939]

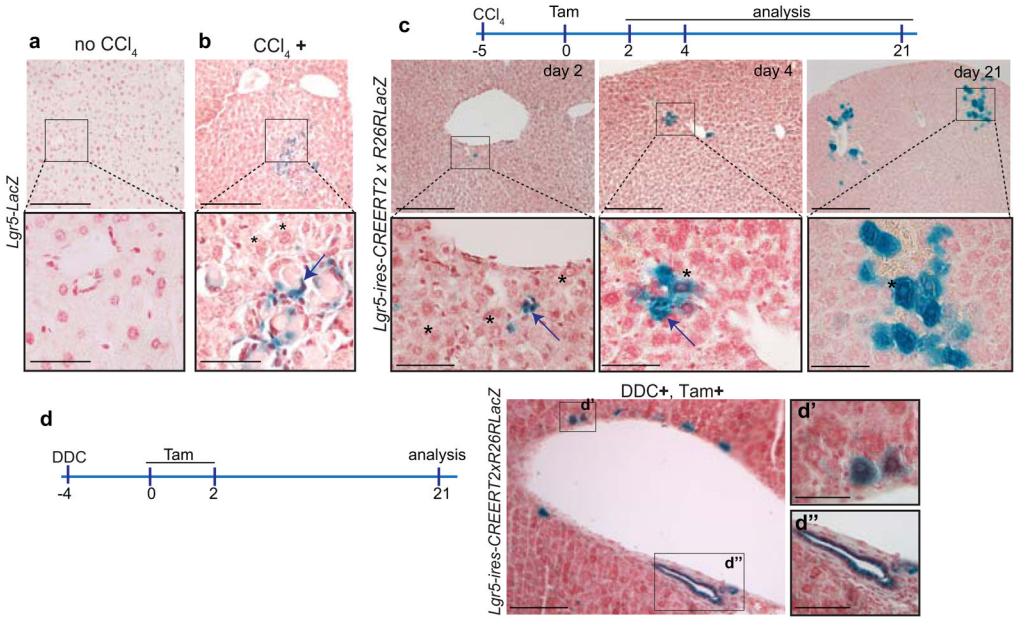

Figure 1. Liver damage induces Lgr5^{+} bi-potential liver progenitors

a–b, *Lgr5-LacZ* mice were injected IP with corn oil (n=6) **(a)** or with a single dose of CCl4 in corn oil (1ml/kg) (n=6) **(b)**. Six days later, mice were sacrificed and livers collected and processed for β-gal staining. **a**, Undamaged liver does not express *Lgr5-LacZ.* **b**, Upon CCl4, strong *Lgr5-LacZ* expression was detected in small cells near ducts. Compare Lgr5-LacZ^{+} cells (arrow) with neighboring hepatocytes (asterisk,*). Scale bars, 200 μm (top panels) and 30 μm (bottom panels). **c**, *Lgr5-ires-CreERT2* mice were crossed with *Rosa26R-LacZ* Cre reporter mice. Offspring received a single IP injection of CCl4 and 2 days later CreERT2 activity was induced with tamoxifen (3mg/mouse) as indicated in the scheme. Representative pictures showing lineage tracing of Lgr5-cells upon CCl4 damage (n=8). Compare differences in size between LacZ^{+} cells (arrows) and hepatocytes (asterisk,*) at days 2 and 4 after tamoxifen induction. Magnifications on each day are the same. Scale bars, 500 μm (top panels) and 50 μm (bottom panels). **d**, *Lgr5-ires-CreERT2* x *Rosa26-LacZ* offspring were fed with DDC (n=3), and 4 and 6 days later CreERT2 activity was induced with tamoxifen as indicated in the scheme. Representative pictures showing positive hepatocytes (**d**′) and positive ductal cells (**d**″). Tam, tamoxifen. Scale bars, 200 μm (**d**), 25 μm (**d**′) and 50 μm (**d**″).

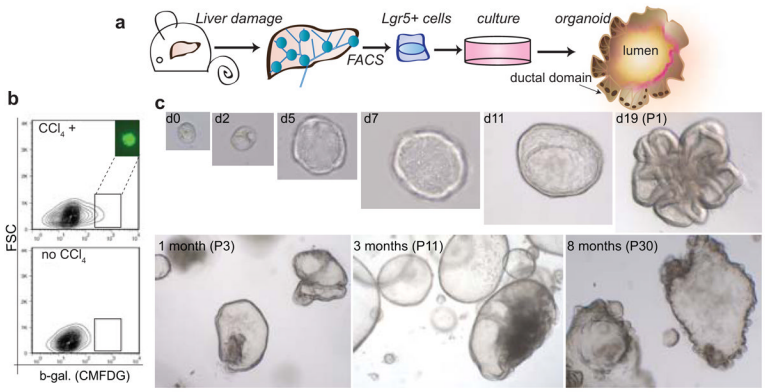

Figure 2. ***In vitro*** **expansion of single Lgr5 cells from adult liver tissue**

a–c, *Lgr5-LacZ* mice were injected with corn oil or CCl4 (IP) as in Fig. 1. Six days later, liver tissue was dissociated to single cells, loaded with the fluorescent CMFDG β-galactosidase substrate and analyzed by FACS. Sorted isolated Lgr5-LacZ+ cells were cultured at a ratio of 1-single *Lgr5-LacZ*$^{+}$ positive cell/well (clonal) as described in Supplementary Methods. **a**, scheme representing the protocol used. **b**, Representative FACS plot of dissociated single cells from CCl4-treated (CCl4+) and non-treated (no CCl4) livers. Cells were gated following sequential selection by cell-size (FSC vs SSC) and PI exclusion. Viable CMFDG^{+} PI^{-} cells were selected and sorted. Representative cell is shown. **c**, Serial DIC images showing the outgrowth of a single *Lgr5-LacZ*$^{+}$ cell. Original magnifications: 40x (days 0–5), 20x (day 7–11), 10x (day 19) and 4x (1 month onwards). P, passage.

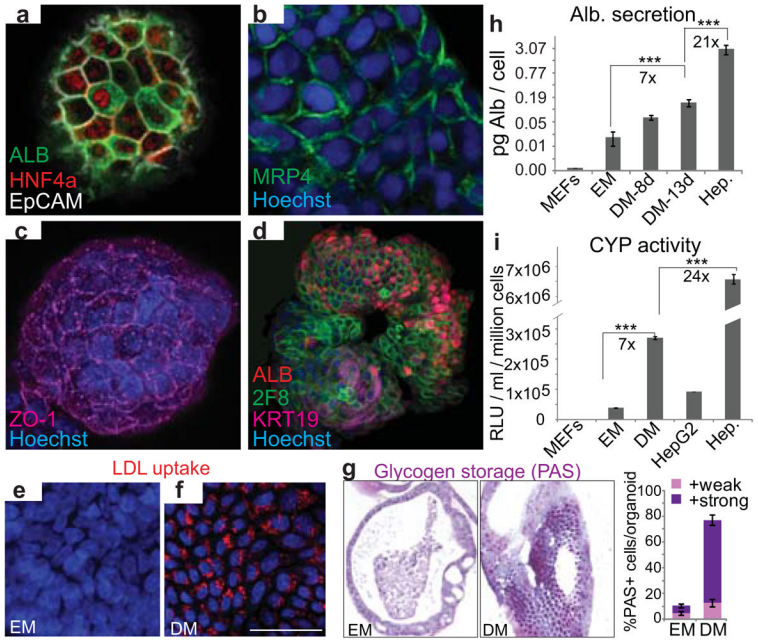

Figure 3. Single cell derived hepatic organoids acquire hepatocyte fate and display hepatocyte functions *in vitro.*

a–i, Clonal Lgr5-derived cultures were grown in expansion medium (EM) and transferred to differentiation medium (DM) for 8–14 days prior to analysis. Two independent clonal cultures were analyzed. **a–d**, confocal images (z-stack projection) for hepatocyte specific markers. **a**, HNF4α (red), albumin (ALB) (green) and EpCAM (grey). **b**, MRP4 (green). **c**, ZO-1 (magenta). **d**, ALB (red) KRT19 (magenta) and hepatocyte surface marker OC2-2F8 (green, full description of OC2-2F8 marker in Supplementary Fig. 8). Nuclei were counterstained with Hoechst. **e–f,** LDL uptake was analyzed using Dil-ac-LDL fluorescent substrate (red) in cultures maintained in EM (**e**) or DM (**f**) for 14 days. Only cultures maintained in DM incorporated the substrate (red). Nuclei were counter-stained with DRAQ5. Scale bar, 50 μm. **g**, Glycogen accumulation was determined by PAS staining in organoids grown in EM or DM for 10 days. Graph shows the percentage of cells weakly or strongly positive for PAS. Results are shown as mean ± SEM of 10 independent sections of 10 EM or 10 DM independent organoids. **h**, Albumin (Alb.) secretion was measured in the 24h supernatant of clonal cultures kept in EM, or DM for 8 days (DM-8d) or 13 days (DM-13d). Results are expressed as pg of albumin per cell. **i,** Cyp3a activity was measured in cultures kept in DM for 13 days. Results are expressed as RLU per ml per million cells. **h–i**, MEFs and Hepatocytes (Hep.) and HepG2 cells were used as negative and positive controls respectively. Triplicates for each condition were analyzed. Results are shown as mean ± SEM of 3 independent experiments. ***, $p<0.0001$.

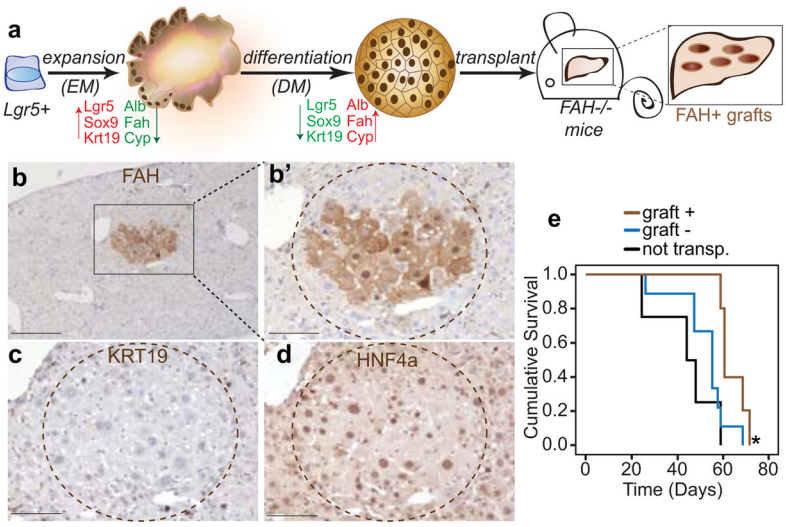

Figure 4. Hepatocyte islands upon transplantation of clonal liver organoids into *FAH*$^{-/-}$-mutant mice

Single-cell derived liver organoids from 3 independent clones were expanded under EM and differentiated for 9 days prior to transplantation into *Fah*$^{-/-}$/*Rag2*$^{-/-}$/*Il2Rγ*$^{-/-}$ (*FRG*) mice. Clone I (n=8), clone II (n=6), clone III (n=5). **a,** scheme showing the transplantation protocol. **b–d,** Representative positive graft within the liver parenchyma. **b**, FAH^{+} area (clone III). The grafted cells were negative for Krt19 (**c,** ductal marker) and positive for HNF4α (**d,** hepatocyte marker). Scale bars, 400μm (**b**) and 100μm (**b′**–**d**). **e,** Kaplan-Meier survival curve of transplanted mice with positive engraftment (brown curve, graft+, n=5), transplanted mice without evidence of engraftment (blue curve, graft-, n=9) and non-transplanted control mice (black curve, not transp., n=4). Plot displays the cumulative survival on a linear scale. Kaplan-Meier survival analysis compares overall survival rates between two groups. Log-rank test is used to compare differences in survival. *, log-rank=0.02 (graft+ *vs* graft-), log-rank= 0.007 (graft+ *vs* not transp.).